Reprogramming CD19-Specific T Cells with IL-21 Signaling Can Improve Adoptive Immunotherapy of B-Lineage Malignancies

Harjeet Singh[1], Matthew J. Figliola[1], Margaret J. Dawson[1], Helen Huls[1], Simon Olivares[1], Kirsten Switzer[1], Tiejuan Mi[1], Sourindra Maiti[1], Partow Kebriaei[2], Dean A. Lee[1,3], Richard E. Champlin[2], and Laurence J.N. Cooper[1,3]

Abstract

Improving the therapeutic efficacy of T cells expressing a chimeric antigen receptor (CAR) represents an important goal in efforts to control B-cell malignancies. Recently an intrinsic strategy has been developed to modify the CAR itself to improve T-cell signaling. Here we report a second extrinsic approach based on altering the culture milieu to numerically expand CAR^+ T cells with a desired phenotype, for the addition of interleukin (IL)-21 to tissue culture improves CAR-dependent T-cell effector functions. We used electrotransfer of *Sleeping Beauty* system to introduce a CAR transposon and selectively propagate CAR^+ T cells on $CD19^+$ artificial antigen-presenting cells (aAPC). When IL-21 was present, there was preferential numeric expansion of CD19-specific T cells which lysed and produced IFN-γ in response to CD19. Populations of these numerically expanded CAR^+ T cells displayed an early memory surface phenotype characterized as $CD62L^+CD28^+$ and a transcriptional profile of naïve T cells. In contrast, T cells propagated with only exogenous IL-2 tended to result in an overgrowth of CD19-specific $CD4^+$ T cells. Furthermore, adoptive transfer of CAR^+ T cells cultured with IL-21 exhibited improved control of $CD19^+$ B-cell malignancy in mice. To provide coordinated signaling to propagate CAR^+ T cells, we developed a novel mutein of IL-21 bound to the cell surface of aAPC that replaced the need for soluble IL-21. Our findings show that IL-21 can provide an extrinsic reprogramming signal to generate desired CAR^+ T cells for effective immunotherapy. *Cancer Res; 71(10); 3516–27. ©2011 AACR.*

Introduction

Adoptive transfer of antigen-specific T cells has been used to treat and prevent malignancies and opportunistic infections. To overcome immune tolerance to human tumor-associated antigens (TAA), investigators have redirected specificity through the introduction of immunoreceptors. An initial clinical trial showed the safety and feasibility of redirecting T cell specificity to CD19, a TAA expressed on B-cell malignancies (1–3). These clinical data demonstrated that infused T cells were short lived due, in part, to the use of a first-generation chimeric antigen receptor (CAR) that recognized CD19 independent of MHC via chimeric CD3-ζ (signal 1). In response, we developed a second-generation CD19-specific CAR to activate T cells through both CD3-ζ and CD28 endodomains (signals 1 and 2, respectively) to improve T-cell activation (4). To translate this CAR to clinical trials, we established a platform for nonviral gene transfer using the *Sleeping Beauty* (SB) system and subsequent selective expansion of CAR^+ T cells recursively cocultured upon $CD19^+$ artificial antigen-presenting cells (aAPC) modified from K562 to express CD19 and desired costimulatory molecules (5–7).

In addition to modifying the CAR itself to augment therapeutic potential, we have now manipulated the tissue culture environment to alter the types of CAR^+ T cells that can be generated. We investigated whether cytokines could be added to cultures to provide a "signal 3" to improve the CAR^+ T cells response to B-cell malignancies.

One attractive cytokine to use in the culturing of T cells is interleukin (IL)-21, which like IL-2, signals through the cytokine receptor common γ chain (IL-2Rγ). This was selected to be tested on the basis of the published work showing that this cytokine increases tumor-specific T cells (8) and/or natural killer (NK) cells (9, 10) leading to antitumor immunity in animal models. Further, IL-21 provides a T-cell survival signal and can act in conjunction with CD28 to support proliferation and acquisition of effector functions (11). T cells genetically modified to have enforced secretion of IL-21 exhibited improved antitumor effect compared to T cells not modified

Authors' Affiliations: [1]Division of Pediatrics, Children's Cancer Hospital, [2]Department of Stem Cell Transplantation and Cellular Therapy, and [3]The University of Texas Graduate School of Biomedical Sciences at Houston, University of Texas MD Anderson Cancer Center, Houston, Texas

Note: Supplementary data for this article are available at Cancer Research Online (http://cancerres.aacrjournals.org/).

Corresponding Author: Laurence J. N. Cooper, University of Texas MD Anderson Cancer Center, Pediatrics-Research, Unit 907, 1515 Holcombe Blvd., Houston, TX 77030. Phone: 713-563-3208; Fax: 713-792-9832; E-mail: ljncooper@mdanderson.org

doi: 10.1158/0008-5472.CAN-10-3843

to secrete cytokines (12). Recombinant soluble IL-21 has been intravenously administered in patients with metastatic renal cell carcinoma, melanoma, and lymphoma, and antitumor activity has been observed (13). In contrast to IL-2, IL-21 also inhibits generation of human regulatory T cells *in vitro* (14).

We hypothesized that altering the culture environment by the addition of IL-21 will lead to improved numeric expansion and functionality of CD19-specific CAR$^+$ T cells. When IL-21 was present with or on aAPC, we found there was a preferential numeric expansion of CAR$^+$ T cells with a preference to propagate subpopulations of (i) CD8$^+$ T cells, (ii) memory T cells, and (iii) naïve T cells, which lysed and produced IFN-γ in response to CD19. This resulted in improved control of CD19$^+$ tumor in a mouse model of human T-cell immunotherapy.

Materials and Methods

Plasmids

The SB transposon $_{CoOp}$CD19RCD28/pSBSO expresses the human codon optimized (CoOp) second generation $_{CoOp}$CD19RCD28 CAR under human elongation factor 1-α (hEF-1α) promoter, flanked by the SB inverted repeats (6). To generate membrane-bound IL-21 (mIL-21), the GM-CSF (granulocyte macrophage-colony-stimulating factor) signal peptide sequence was directly fused to the coding sequence of mature human IL-21 which was attached via a modified [amino acid (aa) 108, Ser → Pro] 12 aa IgG4 hinge region (aa 99–110), to the 5′ end of a human immunoglobulin γ-4 chain C_H2 and C_H3 regions (aa 111–327, UniProtKB P01861), that was fused in frame to human CD4 transmembrane domain (aa 397–418, UniProtKB P01730). After validating the sequence, the human codon optimized cDNA (GENEART) was cloned as a transposon into a SB expression plasmid, pT-MNDU3-eGFP (5) replacing the eGFP sequence to obtain $_{CoOp}$IL-21-Fc/pT-MNDU3 (Fig. 6A). The SB transposase, SB11 is expressed *in cis* from the plasmid pCMV-SB11 (6).

Cell lines and their propagation

Daudi coexpressing β_2-microglobulin (15; Daudiβ_2m, a kind gift from Dr Brian Rabinovich, University of Texas MD Anderson Cancer Center (MDACC)), NALM-6 [pre–B cell; ATCC (American Type Culture Collection)], U251T (glioblastoma; a kind gift from Dr Walder Debinksi, Wake Forest University, NC), CD19$^+$U251T [ref. 6; expressing truncated CD19, ref. 16] were cultured as described previously (5, 6). NALM-6 cells were transduced using a murine stem cell virus–based retroviral vector encoding enhanced firefly luciferase (effLuc; ref. 17) fused with enhanced green fluorescent protein (EGFP; a kind gift from Dr Brian Rabinovich, MDACC). Retrovirus was packaged as previously described (17), concentrated 50× using Amicon Ultra-15 100,000 NMWL centrifugal concentration units (Millipore), mixed with NALM-6 cells in the presence of 8 μg/mL polybrene (Sigma) and spinfected for 90 minutes at 2200 RPM/30°C. One week later, EGFP$^+$NALM-6 cells were sorted on a FACSAria (BD Biosciences). Selective *in vitro* expansion of genetically modified T cells was carried out using K562-derived aAPC (clone no. 4) coexpressing CD19, CD64, CD86, CD137L, and a membrane-bound IL-15 (mIL-15; coexpressed with EGFP; ref. 15). Clone no. 4 was further modified to express mIL-21 using the construct $_{CoOp}$IL-21-Fc/pT-MNDU3. Briefly, 10^6 aAPC were resuspended in 100 μL Amaxa Cell Line Nucleofector Solution V (catalogue no. VPA-1003) along with transposon ($_{CoOp}$IL-21-Fc/pT-MNDU3, 2 μg) and SB transposase (pCMV-SB11, 2 μg) DNA supercoiled plasmids, transferred to a cuvette and electroporated (Program T-16) using Nucleofector II (Lonza). The transfectants were cultured for a week in complete media and a clone (D2) was obtained by plating at limited dilution after FACS (fluorescence-activated cell sorter) sorting. All cell lines were verified by morphology and/or flow cytometry, tested for *Mycoplasma*, and conserved in research cell bank on reception.

Generation of CAR$^+$ T cells

CD19-specific CAR$^+$ T cells were generated from peripheral blood mononuclear cells (PBMC) using SB transposition as previously described and depicted in Figure 1 (5). Briefly, 10^7 to 2×10^7 mononuclear cells, isolated from blood by Ficoll-Paque density gradient centrifugation (GE Healthcare Bio-Sciences AB), were resuspended in 100 μL of Amaxa Nucleofector solution (Human T cell Kit, catalogue no. VPA-1002), along with CAR transposon (CD19RCD28/pSBSO, 15 μg) and SB transposase (pCMV-SB11, 5 μg) DNA plasmids, transferred to a single cuvette and electroporated (Program U-14) on day 0 using Nucleofector II. The cells were rested for 2 to 3 hours at 37°C in incomplete phenol-free RPMI (HyClone) and subsequently cultured overnight in phenol-free RPMI containing 10% FBS and stimulated the next day (day 1) with γ-irradiated (100 Gy) K562-aAPC at a 1:2 T cell/aAPC ratio. Additional γ-irradiated aAPC clone no. 4 were added every 7 days at the same ratio. When used, soluble recombinant human IL-21 (catalogue no. 34-8219-85, eBioscience) was added at a concentration of 30 ng/mL beginning the day after electroporation, and soluble recombinant human IL-2 (IL-2; Chiron) was added to the cultures at 50 U/mL beginning 7 days after electroporation. For experiments where CAR$^+$ T cells were cocultured on mIL-21$^+$ K562-aAPC (T cell/aAPC clone D2 ratio 1:2), IL-2 (50 U/mL) was added to the cultures on day 7 after electroporation. All exogenous cytokines continued to be supplemented on a Monday-Wednesday-Friday schedule for 7-day stimulation cycles marked by the addition of aAPC. The cultures were monitored by flow cytometry for the unwanted presence of a CD3^{neg}CD56$^+$ cell population and if the percentage exceeded approximately 10% of the total population, which usually occurred between 10 and 14 days of initial coculture with aAPC, a depletion for (CD3^{neg}) CD56$^+$ NK cells was carried out using CD56 beads (catalogue no. 130-050-401, Miltenyi Biotech Inc.) on LS column (catalogue no. 130-042-401, Miltenyi Biotech Inc.) according to the manufacturer's instructions. T cells were enumerated every 7 days and viable cells counted based on Trypan blue exclusion using Cellometer automated cell counter (Auto T4 Cell Counter, Nexcelom Bioscience). At the time of electroporation and during the course of coculture, programs "PBMC_human_frozen" and "activated T cell," respectively, were used for counting cells on the Cellometer. The fold expansion (as compared to day 1) of total, CD3$^+$, and CAR$^+$ cells at the end of 7, 14, 28 days of

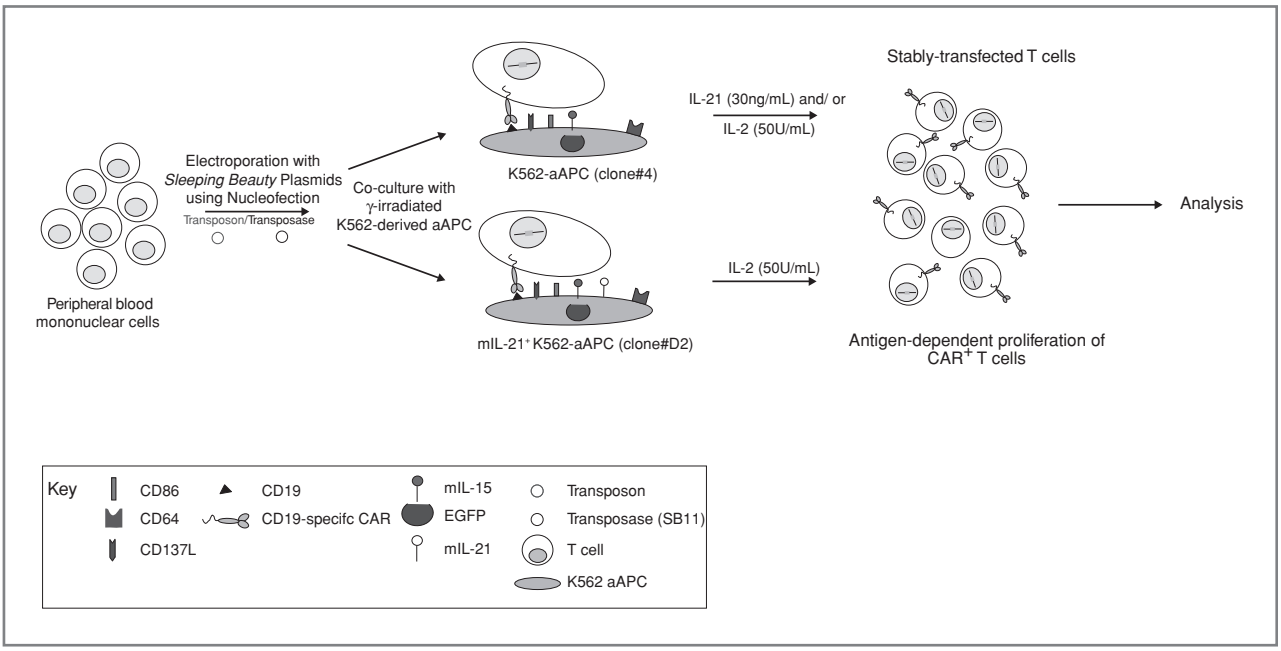

Figure 1. Generation of CAR$^+$ T cells on γ-irradiated aAPC. PBMC were electroporated with SB transposon and transposase. Cells were subsequently cocultured on K562-derived aAPC [modified to coexpress CD19, CD64, CD86, CD137L (4-1BBL), mIL-15, with and without mIL-21] in the presence of soluble IL-21 and/or IL-2.

coculture for individual experiments was calculated and the average compared between culture conditions using a Student's *t* test.

Flow cytometry

Up to 10^6 cells in 100 μL volume were stained with fluorochrome-conjugated [fluorescein isothiocyanate (FITC), phycoerythrin (PE), peridinin chlorophyll protein conjugated to cyanine dye (PerCPCy5.5), allophycocyanin (APC)] reagents which unless otherwise stated, were obtained from BD Biosciences: anti–CD3 FITC (catalogue no. 349201, 5 μL), anti–CD3 PerCPCy5.5 (catalogue no. 340949, 4 μL), anti–CD4 APC (catalogue no. 555349, 2.5 μL), anti–CD8 PerCPCy5.5 (catalogue no. 341051, 4 μL), anti–CD19 PE (catalogue no. 555413, 10 μL), anti–CD28 PerCPCy5.5 (catalogue no. 337181, 4 μL), anti–CD62L APC (catalogue no. 559772, 2.5 μL), anti–CD45RA FITC (catalogue no. 555488, 5 μL), anti–CD45RO APC (catalogue no. 559865, 2.5 μL), anti–IL7Rα Alexa Fluor 647 (catalog no. 558598, 10 μL), anti–PD1 APC (catalogue no. 558694, 2.5 μL), anti–PDL1 PE (catalogue no. 557924, 2.5 μL), anti–NKG2D PE (catalogue no. 557940, 2.5 μL), anti–Granzyme B Alexa Fluor 647 (catalogue no. 560212, 3 μL), anti–Perforin PE (Reagent Set no. 556437, 3 μL), anti–HLA (human leukocyte antigen)-ABC APC (catalogue no. 555555, 2.5 μL), anti–CD86 PE (catalogue no. 555658, 2.5 μL), anti–CD64 PE (catalogue no. 558592, 2.5 μL), anti–CD137L PE (catalogue no. 559446, 2.5 μL), anti–IFN-γ APC (catalogue no. 554702, 2 μL), anti-pSTAT3 (pY705) PE (catalogue no. 612569, 20 μL), anti–IL-21 PE (catalogue no. 12 7219-73, 2.5 μL, eBiosciences), anti–CCR7 PE (catalogue no. FAB197P, 10 μL, R&D Systems) and anti–CXCR4 PE (catalogue no. FAB173P, 10μL, R&D Systems). FITC-conjugated (catalogue no. H10101C, 3 μL, Invitrogen) and PE-conjugated (catalogue no. H10104, 2.5 μL, Invitrogen) F(ab′)$_2$ fragment of goat anti-human Fcγ was used to detect cell surface expression of the CD19-specific CAR. Blocking of nonspecific antibody binding was achieved using FACS wash buffer (2% FBS and 0.1% Sodium azide in PBS). Data acquisition was on a FACSCalibur (BD Biosciences) using CellQuest version 3.3 (BD Biosciences). Analyses and calculation of median fluorescence intensity (MFI) was undertaken using FCS Express version 3.00.007 (Thornhill).

Chromium release assay

The cytolytic activity of T cells was determined in a standard 4-hour chromium release assay (CRA) as described previously (5, 18).

Intracellular IFN-γ production

10^5 T cells were incubated with 0.5×10^6 stimulator cells in 200 μL culture media along with protein transport inhibitor (BD Golgi Plug containing Brefeldin A, catalogue no. 555028) in a round-bottom, 96-well plate. Following a 4 to 6 hour incubation at 37°C, the cells were stained for expression of CAR at 4°C for 30 minutes. After washing, the cells were fixed, permeabilized (for 20 minutes at 4°C with 100 μL of Cytofix/Cytoperm Buffer, catalogue no. 555028) and stained with APC-conjugated monoclonal antibody (mAb) specific for IFN-γ. Cells were further washed and analyzed by FACSCalibur. T cells treated with a leukocyte activation cocktail [PMA (phorbol 12 myristate 13 acetate) and ionomycin, catalogue no. 550583, BD Biosciences] were used as a positive control.

Induction of STAT3 phosphorylation

10^6 CAR$^+$ T cells were incubated with and without aAPC for 30 minutes at 37°C in a V-bottom 96-well plate. The cells were then fixed with 20 excess volumes of 37°C pre-warmed 1 × PhosFlow Lyse/Fix Buffer (catalogue no. 558049, BD

Biosciences) diluted in water at 37°C for 10 minutes to prevent dephosphorylation. Thereafter, pelleted cells were permeabilized by adding BD PhosFlow Perm Buffer III (catalogue no. 55850, BD Biosciences) for 20 minutes on ice, followed by washing with BD Pharmingen Staining Buffer (catalogue no. 554656). Resuspended cells were then stained with antibodies for pSTAT3, CD3, and CAR for 20 minutes in the dark, washed once with BD Pharmingen Staining Buffer, and resuspended in the same buffer for flow cytometry analysis.

nCounter analysis digital gene expression system

Genetically modified T cells (10,000) were lysed in RNeasy lysis buffer (RLT; 5 μL, Qiagen) and frozen for single-use aliquots at −80°C. Lysates were thawed and the selected mRNA content analyzed using the nCounter Analysis System (model no. NCT-SYST-120, NanoString Technologies; ref. 19) after hybridization with a designer reporter code set and capture probe set for 12 hours at 65°C. The probes were designed, synthesized, and hybridized using the nCounter Gene Expression Assay Kit. The posthybridization processing was undertaken using the nCounter Prep Station. Nanominer software was used to carry out normalization compared to internal control and basic statistical analysis on the data. The normalized results are expressed as the relative mRNA level.

In vivo efficacy of CAR$^+$ T cells

On day 0, 7-week-old NOD.Cg-*Prkdc*^{scid}*Il2rg*^{tm1wjl}/SzJ (NSG) mice were intravenously (i.v.) injected via a tail vein with 10^5 EGFP$^+$effLuc$^+$ NALM-6 cells. Mice (n = 5/group) in the 2 treatment cohorts received via tail vein injection (on days 1 and 9) 2×10^7 of CAR$^+$ T cells grown in the presence of IL-2 or CAR$^+$ T cells grown in the presence of IL-2 and IL-21. One group of mice (n = 5) bearing tumor received no T cells. Anesthetized mice underwent bioluminescent imaging (BLI) in an anterior–posterior position using a Xenogen IVIS 100 series system (Caliper Life Sciences) 10 minutes after subcutaneous injection (at neck and shoulder) of 150 μL (200 μg/mouse) freshly thawed aqueous solution of D-Luciferin potassium salt (Caliper Life Sciences) as previously described (20). Photons emitted from NALM-6 xenografts were serially quantified using the Living Image 2.50.1 (Caliper Life Sciences) program. At the end of the experiment, mice were euthanized and tissues harvested. Bone marrow was flushed from the femurs using 30Gx$^1/_2$inch needles (BD, catalogue no. 305106) with 2% FBS in PBS. Spleens were disrupted using a syringe in 2% FBS/PBS and passed through a 40 μm nylon cell strainer (BD, catalogue no. 352340) to obtain single cell suspension. Red blood cells from bone marrow, spleen, and peripheral blood were lysed using ACK lysing buffer (Gibco-Invitrogen, A10492) and remaining cells stained for presence of tumor (CD19 and EGFP) by flow cytometry. Statistical analysis of photon flux and tumor burden was accomplished using Student's t test.

Results

Propagation of CAR$^+$ T cells with IL-21

A master cell-bank of clinical-grade K562-derived aAPC, designated clone no. 4, has been generated through the Production Assistance for Cellular Therapies (PACT) to propagate CD19-specific CAR$^+$ T cells to clinically sufficient numbers. These γ-irradiated aAPC selectively propagate CAR$^+$ T cells after the electrotransfer of SB plasmids coding for CD19RCD28 CAR (5). To investigate extrinsic factors that might improve the therapeutic potential of CAR$^+$ T cells, a role for IL-21 was examined in the culturing process on aAPC. We added this soluble cytokine, in addition to soluble IL-2 and mIL-15 on aAPC, and showed selective expansion of CAR$^+$ T cells (Fig. 2A). This resulted in a greater number of CD3$^+$ and CAR$^+$ T cells at 28 days of coculture on clone no. 4 ($P < 0.05$) compared with T cells receiving IL-2 alone, with differences between the 2 groups already apparent within 2 weeks after electroporation (Fig. 2B and C). Indeed, the average fold expansion of CAR$^+$ T cells at 7 (2.75 ± 1.1 fold, $n = 7$) and 14 (39.2 ± 36.2 fold, $n = 7$) days after electroporation were significantly higher ($P < 0.05$) compared to T cells that only received IL-2 (day 7, 0.29 ± 0.3 fold, $n = 4$; day 14, 0.49 ± 0.36 fold, $n = 4$). After 4 weeks of coculture on aAPC, the group that received IL-21 had an average 19,800 ± 11,313 ($n = 7$) fold expansion of CD3$^+$ T cells and there was a 35,800 ± 23,285 ($n = 7$) fold expansion of CAR$^+$ T cells. In contrast, T cells that only received IL-2 had an average CD3$^+$ fold expansion of 2,280 ± 4,227 ($n = 4$) and CAR$^+$ T cells expanded by an average of 2,680 ± 4,919 ($n = 4$) fold. The average total cell numbers at 7 (4.1×10^7 vs. 4.7×10^6) and 14 (3.1×10^8 vs. 2.7×10^7) days after electroporation were significantly higher ($P < 0.05$) in cultures receiving IL-21, as compared to cultures receiving only IL-2, which was due to an increased average number of average CD3$^+$ T cells (day 7, 4.1×10^7 vs. 3.0×10^6; day 14, 3.5×10^8 vs. 2.4×10^7; $P < 0.05$). These data suggest the addition of soluble recombinant IL-21 to the culture environment augments the propagation of CD3$^+$CAR$^+$ T cells on aAPC clone no. 4.

IL-21 results in qualitative differences in CAR$^+$ T cells

CAR$^+$ T cells cultured only in the presence of IL-2 produced low amounts of IFN-γ in response to CAR binding CD19 and expressed low levels of granzyme B. Expression of this cytokine and granzyme is associated with improved antitumor activity, therefore we investigated whether the presence of IL-21 could augment expression of these factors as T cells were propagated on aAPC. We measured mRNA levels using the nCounter Analysis System and IFN-γ and Granzyme B were found to be significantly elevated in populations of T cells receiving IL-21 (Fig. 3A). At day 28 of culture, we observed a 3-fold increase in IFN-γ (313 vs. 100) and 40-fold increase in granzyme B (4,458 vs. 110) mRNA transcript levels in T cells grown in IL-2 and IL-21, as compared to those grown in soluble IL-2. We demonstrated a significant increase in granzyme B protein levels (mean 89.5% vs. 17%) and CD19-dependent IFN-γ production (mean 55% vs. 0.1%) in the CAR$^+$ T cells receiving IL-21, as compared to those grown in soluble IL-2 (Fig. 3B). Thus, the mRNA measurements are consistent with the phenotype data showing an increase in expression of IFN-γ and granzyme B after coculture of CAR$^+$ T cells with IL-2 and IL-21. We have previously generated CD19RCD28$^+$ T cells on CD19$^+$ aAPC in the presence of soluble IL-2 which tended

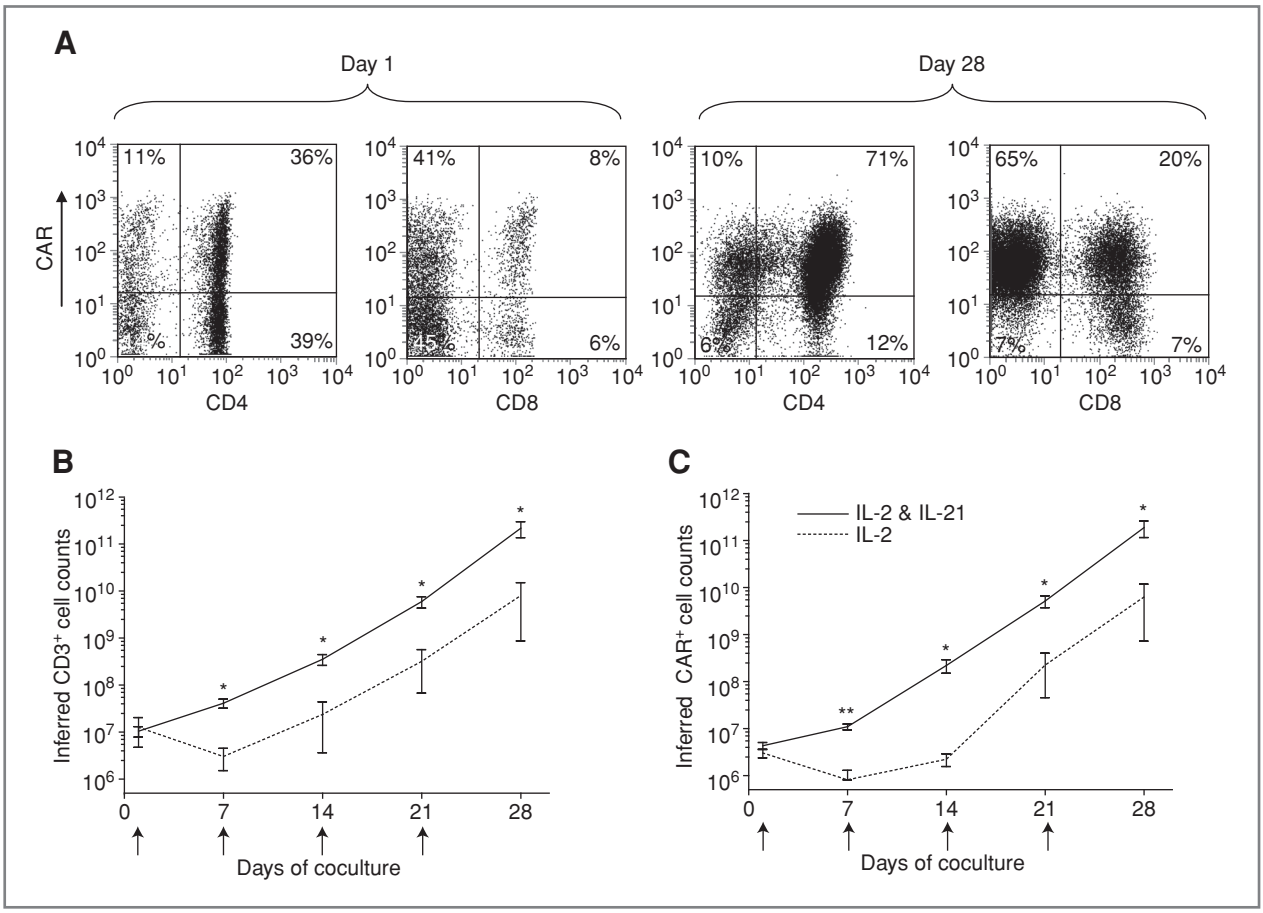

Figure 2. Propagation of genetically modified T cells on aAPC. A, T-cell expression of CAR before and after propagation on aAPC. The rate of T-cell growth cultured on γ-irradiated aAPC for 28 days in the presence of IL-2 ($n = 4$) or IL-2 and IL-21 ($n = 7$). The total number of B, $CD3^+$ cells, and C, CAR^+ T cells propagated over time. Small upward arrows indicate the addition of γ-irradiated aAPC to the culture. Inferred cell counts were calculated assuming all viable cells were carried forward through each stimulation cycle. Mean ± SD is shown; *, $P < 0.05$; **, $P < 0.001$.

to result in a preferential outgrowth of CAR^+ T cells with a predominance of $CD4^+$ T cells (5). Recognizing that $CD8^+$ T cells contribute to antitumor immunity, we sought a method to improve the outgrowth of $CD8^+CAR^+$ T cells on aAPC. IL-21 has been shown to help propagate $CD8^+$ effector T cells (21), therefore the genetically modified T cells were cocultured with aAPC in the presence of exogenous IL-21 and IL-2 for 28 days which resulted in a trend toward improved outgrowth of $CD8^+CAR^+$ compared with $CD4^+CAR^+$ T cells. Day 28 was selected as an endpoint for tissue culture and subsequent analyses since over this time period CAR^+ T cells expand to numbers sufficient for clinical translation (Fig. 2). The T cells receiving IL-21 had 1.8-fold higher number of average $CD8^+$ T cells (24.2 ± 25.3) compared to the T cells receiving just IL-2 (13.4 ± 0.9) at day 28 of coculture (Fig. 3D). At the time of analysis, there was increased CAR expression on the T cells exposed to IL-21 compared to T cells cultured with only IL-2 (mean 90% ± 7.5 vs. 66% ± 7; $P < 0.01$) which indicates that manipulating the cytokine milieu can improve the outgrowth of T cells with increased expression of CAR (Fig. 3C). In aggregate, the addition of IL-21 compared to culturing only with IL-2, results in T cells containing subpopulations that have improved effector function, a trend toward $CD8^+$ phenotype, and augmented CAR expression.

IL-21 results in propagation of subpopulations of CAR^+ T cells with memory and naïve phenotypes

T cells propagated over a prolonged time in tissue culture tend to mature to a differentiated phenotype which may compromise their therapeutic potential. To determine if IL-21 can curtail this differentiation of genetically modified T cells, we examined the expression of (i) eomesodermin (EOMES) which controls cytolytic development and function of T cells, and has recently been shown to be reduced in naïve-derived effector cells (22–24) and (ii) killer cell lectin-like receptor subfamily G, member 1 (KLRG1), an inhibitory receptor that is expressed by senescent T cells (25, 26). At day 28, the T cells cultured only with IL-2 had increased levels of mRNA species coding for EOMES and KLRG1 showing that this cytokine promoted differentiation of CAR^+ T cells on aAPC. However, when IL-21 was added there was a 7-fold and 54-fold reduction in EOMES and KLRG1, respectively (Fig. 3A). To expand on the mRNA data, we examined the cell surface expression for flow

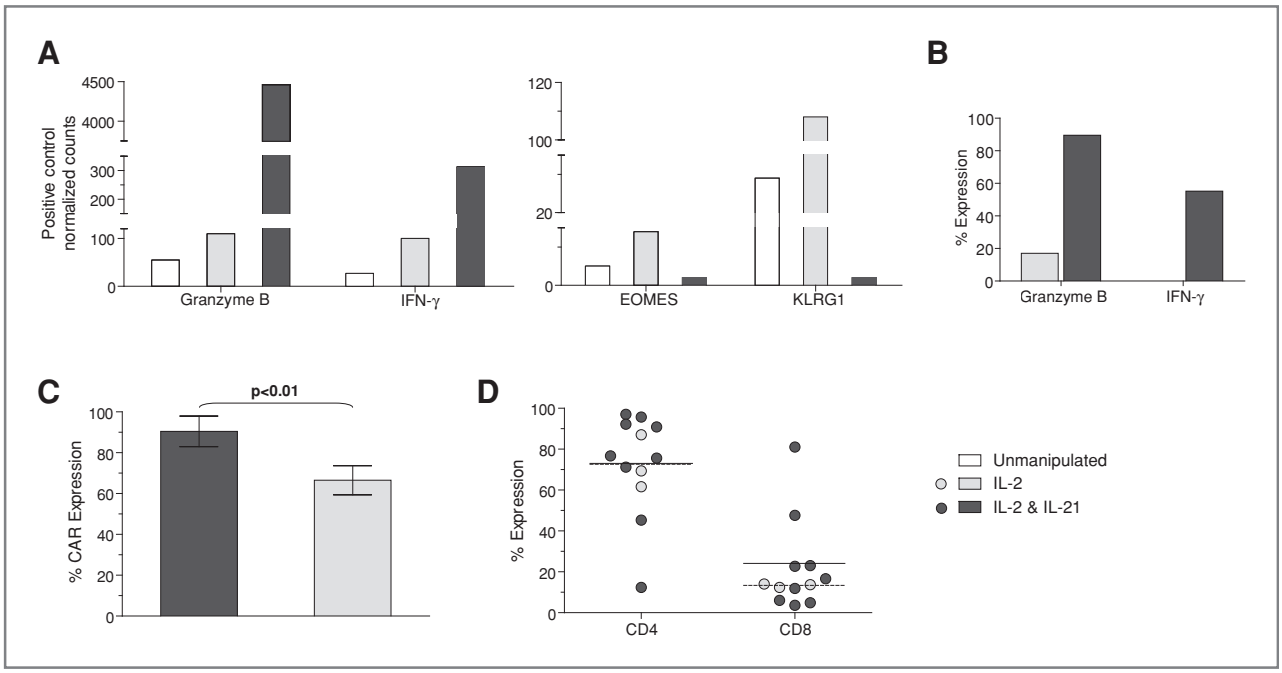

Figure 3. IL-21 supports outgrowth of T cells with improved CAR expression and desired phenotype. CAR$^+$ T cells grown in the presence of IL-2, or IL-21 and IL-2, at the end of 28 days of coculture on aAPC were evaluated for: A, the amount of mRNA transcripts coding for Granzyme B, IFN-γ, EOMES, and KLRG1 using NanoString nCounter analysis, and B, expression of Granzyme B and CD19-specific IFN-γ (percent IFN-γ production when cells were stimulated with CD19$^+$U251T as compared to CD19^{neg} U251T) using flow cytometry. C, total CAR expression (mean ± SD). D, percent CD4 and CD8 T cells in cultures receiving IL-2 and IL-2 & IL-21 at the end of 28 days of coculture over aAPC. Each circle represents individual experiment, horizontal bars represent mean expression, solid (IL-2 and IL-21) and dotted (IL-2).

cytometry markers of naïve, memory, and differentiated T cells. A naïve phenotype was defined by the presence of CD62L and CD45RA, whereas a central memory (T_{CM}) phenotype can be defined by the expression of CD28, CD62L, CCR7, and CD45RO on T cells (27–29). Differentiated effector cells typically lose expression of these markers upon prolonged culturing, and exhausted cells upregulate expression of PD-1 and PDL-1 (30). CAR$^+$ T cells grown in the presence of IL-2 and IL-21 exhibited markers consistent with both naïve and memory cells and lacked expression of PD-1/PDL-1 (Fig. 4A). In addition, the lack of (2%) CD57 expression supports absence of exhaustion among the CAR$^+$ T cells (31). At day 28 of culture, the CAR$^+$ T cells expressed CD28 (mean 69%, range: 22%–88%), CCR7 (mean 16%, range: 0.9%–60.5%), CD62L (mean 50%, range: 22%–75%), CD45RO (93%, range: 84%–98%), and IL7Rα (mean 26%, range: 9%–37%). Among the CAR$^+$ cells were T cells with a T_{CM} phenotype exemplified by the coexpression of CD28$^+$CD62L$^+$ (34%, range: 11%–59%), CD28$^+$CCR7$^+$ (mean 18%, range: 0.8%–56.5%), CD62L$^+$,CCR7$^+$ (10%, range: 0.5%–48%), CD45RO$^+$CD45RA$^+$ (mean 19%, range: 2%–63%). In summary, the addition of IL-21 supports the numeric expansion of CAR$^+$ T cells on aAPC that contain memory and naïve subpopulations.

Redirected specificity of CAR$^+$ T cells numerically expanded with IL-21

T cells expressing CAR and propagated in the presence of IL-2 and IL-21 were able to specifically lyse CD19$^+$ tumor targets (Fig. 4B). At an effector:target ratio of 5:1, the CAR$^+$ T cells could lyse an average 51% (range: 32%–66%) of CD19$^+$ Daudiβ_2m cells and an average 38% (range: 25%–60%) of CD19$^+$ NALM-6. The Daudi cells used as targets were genetically modified to express β_2 microglobulin and thus re-express classical HLA class I (Supplementary Fig. 1) to decrease unwanted killing by contaminating NK or lymphokine-activated killer cells. Specificity for CD19 was shown by a 4.5-fold (range: 1.3–12.6) increased killing of genetically modified CD19$^+$ U251T (glioma) targets as compared to parental CD19^{neg} U251T targets at an effector:target ratio of 5:1. We further assessed the function of CAR$^+$ T cells by evaluating their ability to produce IFN-γ in response to CD19 (Fig. 4C). When CAR$^+$ T cells were stimulated with CD19$^+$ Daudiβ_2m cells there was an average 29.6-fold (range: 4.6–114.9) increase in IFN-γ production. The specificity for production of CD19 was shown by a 12.6-fold (range: 3.2–45.5) increase in IFN-γ production by CAR$^+$ T cells when cocultured with CD19$^+$ U251T cells in comparison to CD19^{neg} U251T cells. These data show that CAR$^+$ T cells cultured in the presence of IL-21 exhibit CD19-dependent redirected effector functions.

Efficacy of CAR$^+$ T cells propagated on aAPC to treat B-lineage malignancy

We investigated whether CAR$^+$ T cells numerically expanded in the presence of IL-2 and IL-21 were able to show an improved antitumor effect compared with CAR$^+$ T cells cultured with only IL-2. Mice injected with NALM-6 were longitudinally measured by BLI for tumor-associated effLuc activity. We observed that CAR$^+$ T cells grown in the presence

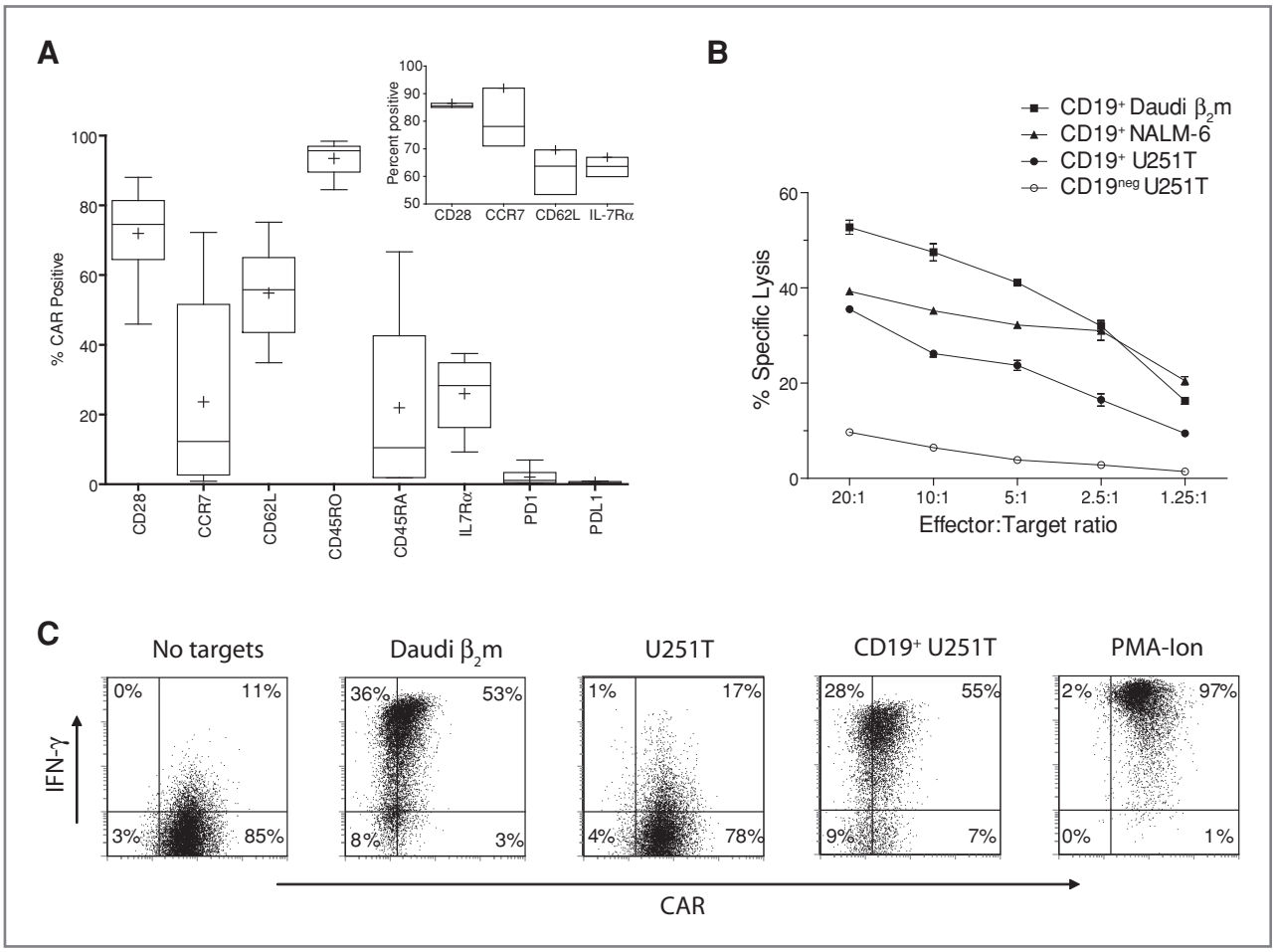

Figure 4. IL-21 supports outgrowth of sub-populations of naïve and memory CD19-specific CAR$^+$ T cells. A, immunophenotype of genetically modified T cells numerically expanded in the presence of IL-2 and IL-21. Inset shows expression of selected cell-surface proteins before electroporation on T cells obtained from PBMC ($n = 3$). Data are presented as "Box-and-Whiskers" plot and in inset as "low-high-bar" plot. Horizontal bar within boxes represents median and "+" represents the means. B, four-hour CRA shows killing of CD19$^+$ Daudiβ_2m, NALM-6, and CD19$^+$U251T cells. Lysis of CD19^{neg}U251T cells demonstrates background killing. Mean $\pm$ SD for triplicate wells is represented. C, IFN-γ production by CAR$^+$ T cells upon incubation with targets. PMA-ionomycin is used as a positive control.

of IL-2 and IL-21 were more effective in controlling tumor growth as compared to CAR$^+$ T cells grown in the presence of IL-2 (day 8, $P < 0.01$; day 13, $P < 0.05$; day 17, $P < 0.05$) and as compared to mice that did not receive T cells (days 8, 13, 17, $P < 0.01$; Fig. 5A and B). Groups of mice receiving no T cells or CAR$^+$ T cells grown in the presence of IL-2 showed similar rates of tumor growth (day 8, $P = 0.11$; day 13, $P = 0.2$; day 17, $P = 0.07$). Tissues from mice were assessed for EGFP$^+$CD19$^+$ NALM-6 and consistent with the BLI data, we observed that the tumor burden was significantly reduced in mice receiving CAR$^+$ T cells grown in the presence of IL-2 and IL-21, as compared to mice receiving no T cells or CAR$^+$ T cells grown in the presence of IL-2 (Fig. 5C and D). The presence of NALM-6 blasts in peripheral blood was lower in the IL-2 and IL-21 (1.8 $\pm$ 0.92, mean $\pm$ SD) group as compared to mice that received CAR$^+$ T cells cultured with IL-2 (20.4 $\pm$ 20.3, $P < 0.05$) or no T cells (3.8 $\pm$ 0.6, $P < 0.01$). There was also a significant reduction in average tumor burden in the bone marrow after administration of T cells that were cultured with IL-2 and IL-21 group (48.5 $\pm$ 4.2) as compared to IL-2 group (86.6 $\pm$ 7.8, $P < 0.00001$) or no T-cell group (86.6 $\pm$ 7.9, $P < 0.001$). The difference in average splenic tumor burden was more apparent ($P < 0.0001$) comparing mice that received CAR$^+$ T cells cultured with IL-2 and IL-21 (30.9 $\pm$ 18.8) vs. mice that were infused with CAR$^+$ cells cultured with IL-2 (88.3 $\pm$ 4). The tumor burden was similar in the blood ($P = 0.07$) and bone marrow ($P = 0.49$) between the mice that received no T cells and mice that received CAR$^+$ T cells cultured with IL-2. Thus, these *in vivo* data confirm that CD19-specific CAR$^+$ cells propagated on aAPC in presence of IL-2 and IL-21 are superior in controlling tumor growth.

A membrane-bound mutein of IL-21 can replace soluble recombinant IL-21

Signaling through 2nd generation CAR and cytokine receptor(s) occurs in the tissue culture environment enabling aAPC to selectively propagate T cells that receive signals 1, 2, and 3. To improve the coordination between these sig-

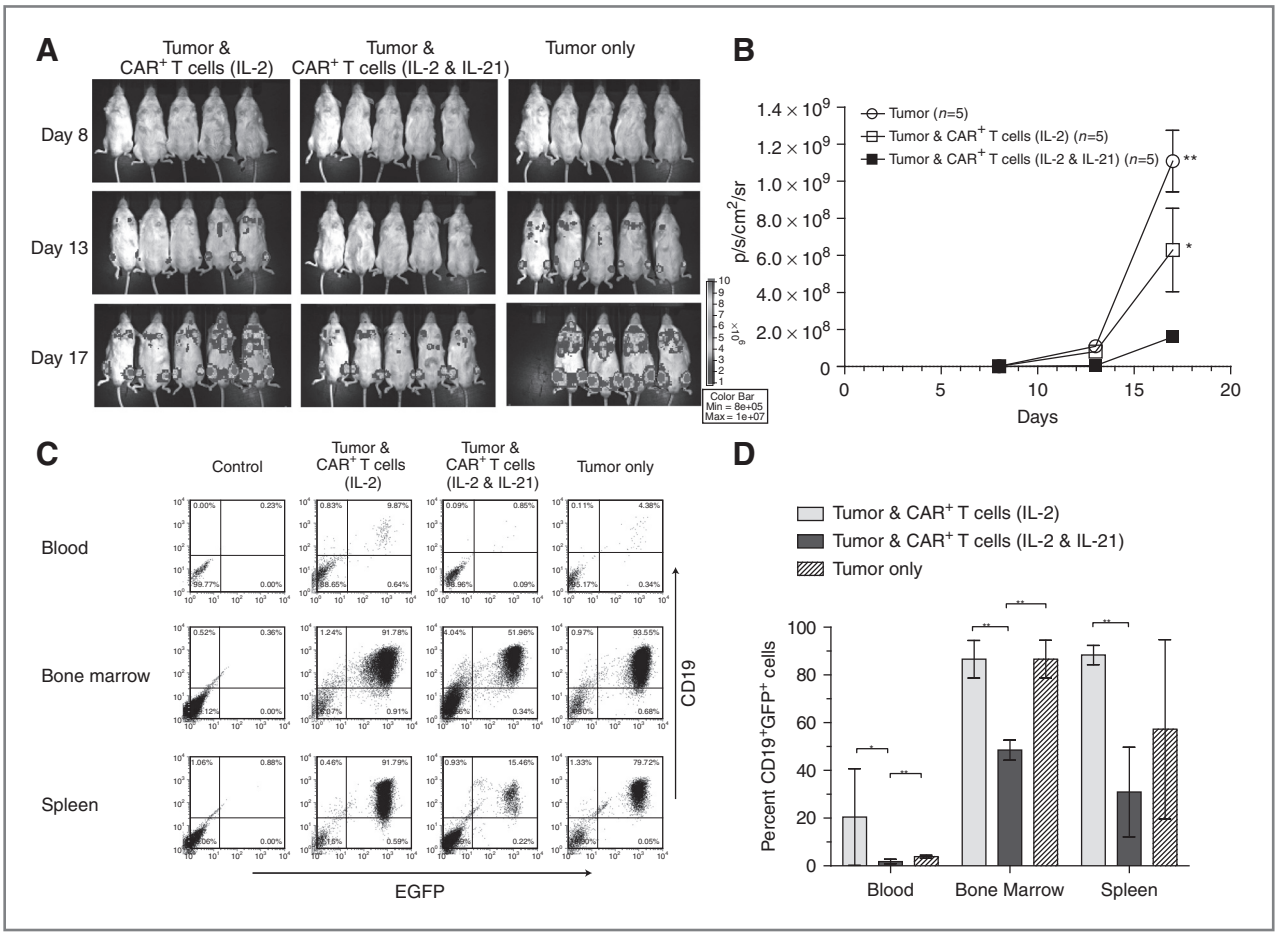

Figure 5. Efficacy of CAR$^+$ T cells in mice. NSG mice i.v. injected (day 0) with 10^5 EGFP$^+$effLuc$^+$ NALM-6 tumor received, on days 1 and 9, 2×10^7 CAR$^+$ T cells grown in the presence of IL-2 or IL-2 & IL-21, or received no T cells. A, false-colored images representing photon flux from NALM-6–derived ffLuc activity. B, time course of longitudinal measurements of tumor-derived mean photon flux $\pm$ SD from 3 groups of mice ($n = 5$). Background luminescence (10^6 p/s/cm^2/sr) was defined from mice with no tumor imaged after receiving D-Luciferin in parallel with mice in treatment groups. *In vitro* ffLuc-derived activity of genetically modified EGFP$^+$effLuc$^+$ NALM-6 was 2.8 $\pm$ 0.2 cpm/cell (mean $\pm$ SD) compared with 0.003 $\pm$ 0.001 cpm/cell (mean $\pm$ SD) for parental NALM-6 cells that do not express ffLuc. C, at the end of the experiment (day 21) mice were euthanized and tissues (blood, bone marrow, spleen) were harvested and analyzed by flow cytometry for expression of CD19 and EGFP. Representative flow cytometry dot plots for tumor at various sites are shown. E, the percentage of CD19$^+$EGFP$^+$ cells present in mice from the 3 groups (mean $\pm$ SD) is shown along with statistical significance (*, $P < 0.05$, **, $P < 0.01$).

nals, we altered the aAPC to not only provide the CD19 antigen and associated costimulatory molecules, but to express a novel mutein of membrane-bound of IL-21 (Fig. 6A). This enabled us to test the hypothesis that expressing IL-21 on the cell surface of the aAPC could replace the need for providing IL-21 as a soluble recombinant cytokine. To accomplish this, the aAPC clone no. 4 were electroporated with the SB plasmid $_{CoOp}$IL-21-Fc/pT-MNDU3 and a subclone (D2) was selected based on uniform expression of mIL-21 and the other introduced cell surface markers (Fig. 6B). PBMC electroporated with SB system to express CD19R-CD28 and propagated on γ-irradiated mIL-21$^+$ aAPC in the absence of soluble IL-21, but in the presence of soluble IL-2 resulted in an outgrowth of CAR$^+$ T cells (Fig. 7A). The CAR expression (81% vs. 79%) was similar to when T cells were grown in the presence of exogenous IL-21 or with aAPC expressing mIL-21. The average fold expansion at the end of 28 days of coculture as assessed by expression of CD3 (11,700; $P = 0.27$, not significant, NS) and CAR (14,000; $P = 0.17$, NS) on T cells numerically expanded with mIL-21$^+$ aAPC was similar to the T cells propagated with soluble IL-21 (Fig. 7B). The CAR$^+$ T cells numerically expanded on mIL-21$^+$ aAPC showed specific lysis of CD19$^+$ target cells and a 13-fold increase in IFN-γ production when cells were stimulated with CD19$^+$ U251T targets over control CD19^{neg}U251T cells (Fig. 7D). To examine if mIL-21 can directly activate T cells, we evaluated the phosphorylation status of STAT3. CAR$^+$ T cells that were propagated for 28 days with IL-2 plus mIL-21^{neg} aAPC (clone no. 4) and IL-2 plus mIL-21$^+$ aAPC (clone no. D2), were stimulated for 30 minutes on aAPC with (clone no. D2) or without mIL-21 (clone no. 4). T cells cultured with IL-2 and soluble IL-21 stimulated with aAPC (clone no. 4) along with soluble IL-21 were used as positive controls. CAR$^+$ T cells cultured on mIL-21$^+$ aAPC in

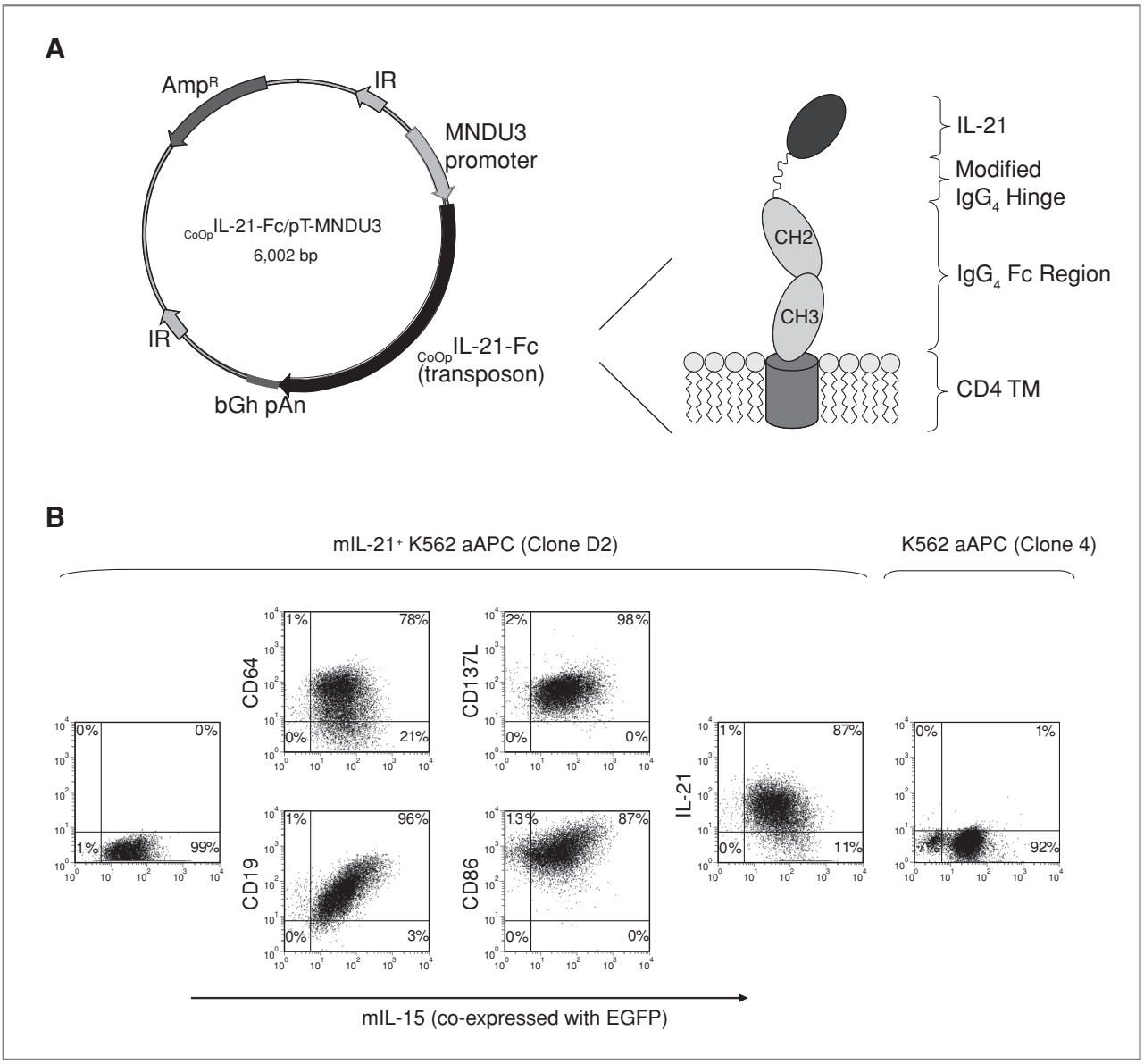

Figure 6. Expression of membrane-bound IL-21 (mIL-21). A, schematic of the DNA plasmid, $_{CoOp}$IL-21-Fc/pT-MNDU3, expressing mIL-21 along with a cartoon showing the folded mIL-21 protein. Abbreviations: MNDU3 promoter, promoter from U3 region of the MND retrovirus; $_{CoOp}$IL-21-Fc, codon-optimized mIL-21 (IL-21-Fc fusion); IR, SB-inverted/direct repeats; bGh pAn, polyadenylation signal from bovine growth hormone; Amp^R, ampicillin resistance gene. B, dot plots showing the presence of mIL-21 (detected by mAb against IL-21) and cell surface markers (CD19, CD64, CD86, CD137, mIL-15) on the aAPC.

the presence of IL-2 when stimulated with mIL-21$^+$ aAPC resulted in an increase in MFI of pSTAT3 (27.1), over the unstimulated control T cells (11.6), or when stimulated with aAPC lacking mIL-21 (13.2; Fig. 7C). When CAR$^+$ T cells which had been propagated on aAPC (clone no. 4) in the presence of IL-2 (and had not seen IL-21 in any form) were exposed to mIL-21$^+$ aAPC, there was a similar increase in MFI of pSTAT3 (25.2) compared to the controls (unstimulated, 11.1; aAPC lacking mIL-21, 14.3). These data show that mIL-21 on aAPC is functional and capable of activating T cells through the STAT3 pathway. In aggregate, these data suggest that mIL-21$^+$ aAPC can replace soluble recombinant IL-21 to selectively propagate CAR$^+$ T cells with redirected specificity.

Discussion

The tissue culture environment can be modified to play a critical role in the growth and function of T cells propagated *in vitro*. In the current study, we show that the addition of IL-21 to the culture milieu in soluble form or presented in conjunction with antigen on aAPC results in improved effector function and preservation of naïve/memory phenotype of CAR$^+$ T cells which predicts for improved therapeutic effect in clinical trials.

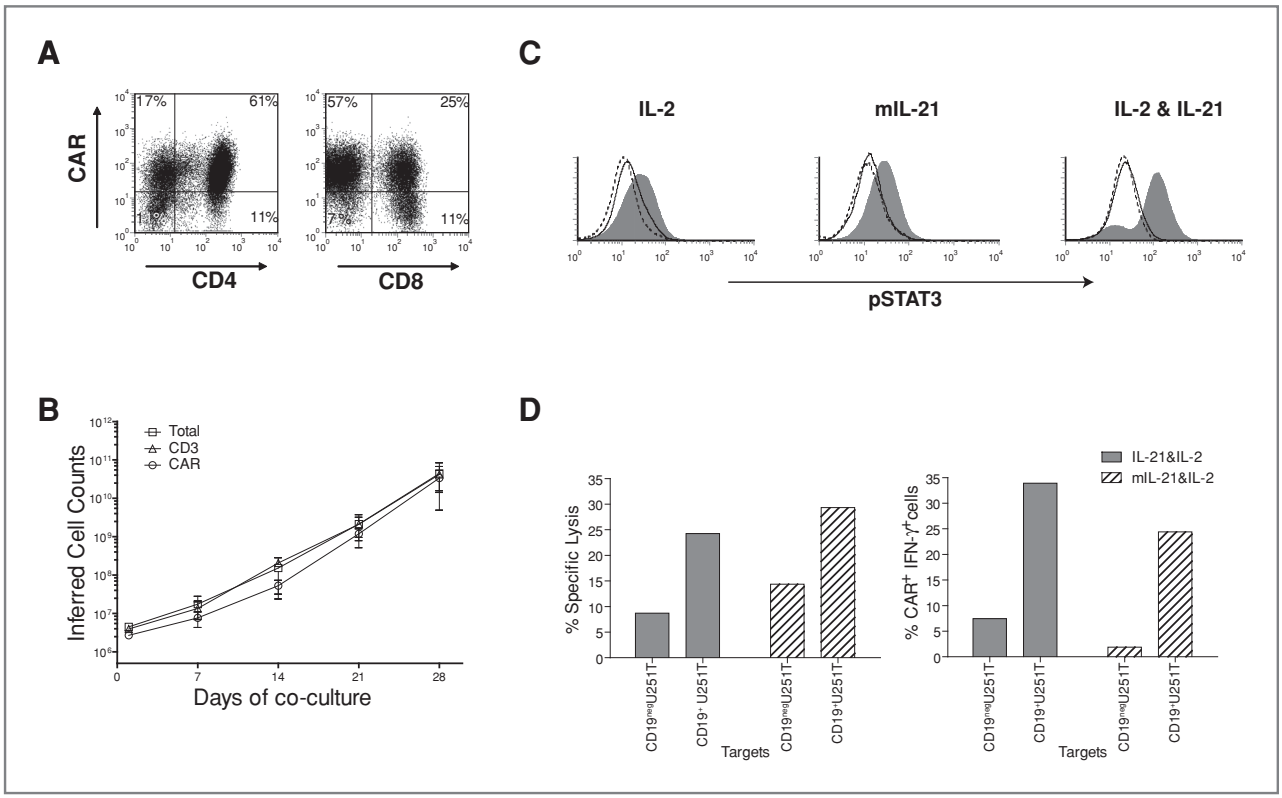

Figure 7. Characterization of T cells grown on mIL-21$^+$ aAPC. A, CAR expression on CD4$^+$ and CD8$^+$ T cells after 28 days of coculture on mIL-21$^+$ aAPC (clone no. D2) along with exogenous IL-2. B, expansion of total, CD3$^+$, and CAR$^+$ T cells over 28 days of culture period. C, induction of STAT3 phosphorylation was measured in T cells grown with IL-2 or mIL-21 & IL-2. These propagated T cells were subsequently stimulated by aAPC with (Clone D2, filled grey histograms) or without (Clone 4, black histograms) mIL-21 for 30 minutes, then fixed, permeabilized, and stained for flow cytometry. Cells grown in presence of IL-2 and soluble IL-21 stimulated with aAPC (Clone 4) with (filled grey histogram) and without (black histogram) soluble IL-21 were used as control. Histograms (dotted, unstimulated cells) represent phosphoSTAT3 staining and indicate a shift in MFI. D, redirected specificity of CAR$^+$ T cells grown on mIL-21$^+$ aAPC with IL-2 as measured by 4-hour CRA and flow cytometry for IFN-γ production.

Initial (first generation) CARs commonly link a scFv to a single signaling moiety (e.g., CD3-ζ) and these typically showed a lack of sustained persistence *in vivo* (2). Therefore, the CAR design was modified to add one or more costimulatory signaling domains of CD28 (4), 4-1BB (32, 33), OX40 (34) to generate "second" or "third" generation CARs. We have previously described our second generation CAR, CD19RCD28, which provides CD19-dependent signaling through CD3ζ and CD28 resulting in improved persistence and antitumor effect (4). Operating under the premise that T cells propagated in a CAR-dependent manner *ex vivo* may select for T cells with sustained proliferation *in vivo*, we developed a culturing system based on aAPC to selectively numerically expand CAR$^+$ T cells. Such aAPC derived from K562 can be tailored to express cell-surface antigen (35) or intracellular antigen presented by restricting MHC (36, 37) in the context of desired and introduced T-cell costimulatory molecules (37–40). Our aAPC (clone no. 4) were also engineered to express mIL-15 and this membrane-bound cytokine is present throughout our culturing process in addition to the addition of soluble cytokines. The addition of IL-21–mediated signaling during the culturing process to selectively propagate T cells expressing a second generation CD19-specific CAR resulted in an outgrowth of T cells on aAPC with a desired phenotype and improved function when assessed *in vitro* and *in vivo*. Thus, from the perspective of manufacturing CAR$^+$ T cells for clinical application it appears beneficial to include IL-21 in the culturing process.

It has been previously shown that the tissue culture microenvironment can be altered with cytokines for improved T-cell function. For example, T cells can be primed using cytokines to augment immune responses after adoptive transfer. In some cases, this is dependent on generation of memory phenotype which requires the presence of IL-15 and IL-21 (41, 42). This memory phenotype predicts for improved persistence as shown for T cells cultured with IL-7, IL-15, and IL-21, compared to T cells propagated with IL-2 (8, 43, 44). Our data provide supportive evidence that not only can the CAR be manipulated, but the choice of additional cytokines influences the number and character of the propagated CAR$^+$ T cells.

Membrane-bound cytokines (45, 46) offer an attractive approach for delivering a desired cytokine to the immediate microenvironment of the T cell-aAPC synapse along with alleviating the need to add the soluble recombinant (expensive) cytokine to the culture system and avoiding the need to procure clinical-grade cytokine for clinical applications. Membrane-bound IL-15 has been used to propagate

T cells (6, 47) and NK cells (48, 49) on aAPC derived from K562 cells. Our aAPC (clone no. 4) used in this study express mIL-15 and is being used in our clinical trials infusing patient- and donor-derived CD19-specific CAR^+ T cells after autologous and allogeneic hematopoietic stem-cell transplantation. Building upon the success of aAPC expressing mIL-15, we further modified the aAPC clone no. 4 to coexpress mIL-21 and suggest that this genetic approach to aAPC design may avoid the need to add soluble recombinant IL-21 to the culture.

Our data show that the SB system and aAPC platform can be manipulated to culture T cells to receive 3 coordinated signals. This was achieved by influencing intrinsic (CAR) and now extrinsic (tissue culture) factors to improve the therapeutic potential of genetically modified and propagated T cells. Activation through second generation CAR, triggered by CD3ζ (signal 1) and CD28 (signal 2), and common γ_c receptor (triggered by IL-21, signal 3) results in generation of CAR^+ T cells that have an improved ability to respond to CD19 compared to T cells cultured without IL-21. The ability to augment signal 3 leads to an outgrowth of CAR^+ T cells on aAPC that have desired properties for use in clinical trials.

Disclosure of Potential Conflicts of Interest

No potential conflicts of interest were disclosed.

Acknowledgments

The authors thank Karen Ramirez and David He from Flow Cytometry Core Laboratory (NIH grant no. 5P30CA016672-32) for their help with flow cytometry. The authors also thank Brian Rabinovich for assistance with transduction of NALM-6 tumor cells.

Grant Support

The work was supported by Cancer Center Core Grant (CA16672); DOD PR064229; PO1 (CA100265); RO1 (CA124782, CA120956, CA141303); R33 (CA116127); Mr. and Mrs. Joe H. Scales; The Alex Lemonade Stand Foundation; The Burroughs Wellcome Fund; The Cancer Prevention Research Institute of Texas; The Gillson Longenbaugh Foundation; The Harry T. Mangurian Jr, Foundation, The Institute of Personalized Cancer Therapy; The Leukemia and Lymphoma Society; The Lymphoma Research Foundation; The Miller Foundation; The National Foundation for Cancer Research; The Pediatric Cancer Research Foundation; and The William Lawrence and Blanche Hughes Children's Foundation.

The costs of publication of this article were defrayed in part by the payment of page charges. This article must therefore be hereby marked *advertisement* in accordance with 18 U.S.C. Section 1734 solely to indicate this fact.

Received October 20, 2010; revised March 9, 2011; accepted March 15, 2011; published OnlineFirst May 10, 2011.

References

1. Jensen MC, Popplewell L, DiGiusto DL, Kalos M, Cooper L JN, Raubitschek A, et al. A first-in-human clinical trial of adoptive therapy using CD19-specific chimeric antigen receptor re-directed T cells for recurrent/refrctory follicular lymphoma. Mol Ther 2007; 15:S142.
2. Jensen MC, Popplewell L, Cooper LJ, DiGiusto D, Kalos M, Ostberg JR, et al. Antitransgene rejection responses contribute to attenuated persistence of adoptively transferred CD20/CD19-specific chimeric antigen receptor redirected T cells in humans. Biol Blood Marrow Transplant 2010;16:1245–56.
3. Jena B, Dotti G, Cooper LJ. Redirecting T-cell specificity by introducing a tumor-specific chimeric antigen receptor. Blood 2010;116: 1035–44.
4. Kowolik CM, Topp MS, Gonzalez S, Pfeiffer T, Olivares S, Gonzalez N, et al. CD28 costimulation provided through a CD19-specific chimeric antigen receptor enhances *in vivo* persistence and antitumor efficacy of adoptively transferred T cells. Cancer Res 2006;66:10995–1004.
5. Singh H, Manuri PR, Olivares S, Dara N, Dawson MJ, Huls H, et al. Redirecting specificity of T-cell populations for CD19 using the Sleeping Beauty system. Cancer Res 2008;68:2961–71.
6. Davies JK, Singh H, Huls H, Yuk D, Lee DA, Kebriaei P, et al. Combining CD19 redirection and alloanergization to generate tumor-specific human T cells for allogeneic cell therapy of B-cell malignancies. Cancer Res 2010;70:3915–24.
7. Hackett PB, Largaespada DA, Cooper LJ. A transposon and transposase system for human application. Mol Ther 2010;18:674–83.
8. Moroz A, Eppolito C, Li Q, Tao J, Clegg CH, Shrikant PA. IL-21 enhances and sustains $CD8^+$ T cell responses to achieve durable tumor immunity: comparative evaluation of IL-2, IL-15, and IL-21. J Immunol 2004;173:900–9.
9. Ma HL, Whitters MJ, Konz RF, Senices M, Young DA, Grusby MJ, et al. IL-21 activates both innate and adaptive immunity to generate potent antitumor responses that require perforin but are independent of IFN-gamma. J Immunol 2003;171:608–15.
10. Brady J, Hayakawa Y, Smyth MJ, Nutt SL. IL-21 induces the functional maturation of murine NK cells. J Immunol 2004;172:2048–58.
11. Casey KA, Mescher MF. IL-21 promotes differentiation of naive CD8 T cells to a unique effector phenotype. J Immunol 2007;178: 7640–8.
12. Markley JC, Sadelain M. IL-7 and IL-21 are superior to IL-2 and IL-15 in promoting human T cell-mediated rejection of systemic lymphoma in immunodeficient mice. Blood 2010;115:3508–19.
13. Hashmi MH, Van Veldhuizen PJ. Interleukin-21: updated review of Phase I and II clinical trials in metastatic renal cell carcinoma, metastatic melanoma and relapsed/refractory indolent non-Hodgkin's lymphoma. Expert Opin Biol Ther 2010;10:807–17.
14. Li Y, Yee C. IL-21 mediated Foxp3 suppression leads to enhanced generation of antigen-specific $CD8^+$cytotoxic T lymphocytes. Blood 2008;111:229–35.
15. Manuri PV, Wilson MH, Maiti SN, Mi T, Singh H, Olivares S, et al. piggyBac transposon/transposase system to generate CD19-specific T cells for the treatment of B-lineage malignancies. Hum Gene Ther 2010;21:427–37.
16. Serrano LM, Pfeiffer T, Olivares S, Numbenjapon T, Bennitt J, Kim D, et al. Differentiation of naive cord-blood T cells into CD19-specific cytolytic effectors for posttransplantation adoptive immunotherapy. Blood 2006;107:2643–52.
17. Rabinovich BA, Ye Y, Etto T, Chen JQ, Levitsky HI, Overwijk WW, et al. Visualizing fewer than 10 mouse T cells with an enhanced firefly luciferase in immunocompetent mouse models of cancer. Proc Natl Acad Sci U S A 2008;105:14342–6.
18. Cooper LJ, Topp MS, Serrano LM, Gonzalez S, Chang WC, Naranjo A, et al. T-cell clones can be rendered specific for CD19: toward the selective augmentation of the graft-versus-B-lineage leukemia effect. Blood 2003;101:1637–44.
19. Geiss GK, Bumgarner RE, Birditt B, Dahl T, Dowidar N, Dunaway DL, et al. Direct multiplexed measurement of gene expression with color-coded probe pairs. Nat Biotechnol 2008;26:317–25.
20. Singh H, Serrano LM, Pfeiffer T, Olivares S, McNamara G, Smith DD, et al. Combining adoptive cellular and immunocytokine therapies to improve treatment of B-lineage malignancy. Cancer Res 2007;67: 2872–80.
21. Li Y, Bleakley M, Yee C. IL-21 influences the frequency, phenotype, and affinity of the antigen-specific CD8 T cell response. J Immunol 2005;175:2261–9.
22. Pearce EL, Mullen AC, Martins GA, Krawczyk CM, Hutchins AS, Zediak VP, et al. Control of effector $CD8^+$ T cell function by the transcription factor Eomesodermin. Science 2003;302:1041–3.

23. Intlekofer AM, Takemoto N, Wherry EJ, Longworth SA, Northrup JT, Palanivel VR, et al. Effector and memory CD8$^+$ T cell fate coupled by T-bet and eomesodermin. Nat Immunol 2005;6:1236–44.
24. Hinrichs CS, Borman ZA, Gattinoni L, Yu Z, Burns WR, Huang J, et al. Human effector CD8$^+$ T cells derived from naive rather than memory subsets possess superior traits for adoptive immunotherapy. Blood 2011;117:808–14.
25. Henson SM, Franzese O, Macaulay R, Libri V, Azevedo RI, Kiani-Alikhan S, et al. KLRG1 signaling induces defective Akt (ser473) phosphorylation and proliferative dysfunction of highly differentiated CD8$^+$ T cells. Blood 2009;113:6619–28.
26. Voehringer D, Koschella M, Pircher H. Lack of proliferative capacity of human effector and memory T cells expressing killer cell lectinlike receptor G1 (KLRG1). Blood 2002;100:3698–702.
27. Dutton RW, Bradley LM, Swain SL. T cell memory. Annu Rev Immunol 1998;16:201–23.
28. Sallusto F, Lenig D, Forster R, Lipp M, Lanzavecchia A. Two subsets of memory T lymphocytes with distinct homing potentials and effector functions. Nature 1999;401:708–12.
29. Sallusto F, Geginat J, Lanzavecchia A. Central memory and effector memory T cell subsets: function, generation, and maintenance. Annu Rev Immunol 2004;22:745–63.
30. Barber DL, Wherry EJ, Masopust D, Zhu B, Allison JP, Sharpe AH, et al. Restoring function in exhausted CD8 T cells during chronic viral infection. Nature 2006;439:682–7.
31. Brenchley JM, Karandikar NJ, Betts MR, Ambrozak DR, Hill BJ, Crotty LE, et al. Expression of CD57 defines replicative senescence and antigen-induced apoptotic death of CD8$^+$ T cells. Blood 2003;101:2711–20.
32. Imai C, Mihara K, Andreansky M, Nicholson IC, Pui CH, Geiger TL, et al. Chimeric receptors with 4–1BB signaling capacity provoke potent cytotoxicity against acute lymphoblastic leukemia. Leukemia 2004;18:676–84.
33. Brentjens RJ, Santos E, Nikhamin Y, Yeh R, Matsushita M, La Perle K, et al. Genetically targeted T cells eradicate systemic acute lymphoblastic leukemia xenografts. Clin Cancer Res 2007;13:5426–35.
34. Pulè MA, Straathof KC, Dotti G, Heslop HE, Rooney CM, Brenner MK. A chimeric T cell antigen receptor that augments cytokine release and supports clonal expansion of primary human T cells. Mol Ther 2005;12:933–41.
35. Numbenjapon T, Serrano LM, Singh H, Kowolik CM, Olivares S, Gonzalez N, et al. Characterization of an artificial antigen-presenting cell to propagate cytolytic CD19-specific T cells. Leukemia 2006;20:1889–92.
36. Latouche JB, Sadelain M. Induction of human cytotoxic T lymphocytes by artificial antigen-presenting cells. Nat Biotechnol 2000;18:405–9.
37. Hirano N, Butler MO, Xia Z, Berezovskaya A, Murray AP, Ansén S, et al. Efficient presentation of naturally processed HLA class I peptides by artificial antigen-presenting cells for the generation of effective antitumor responses. Clin Cancer Res 2006;12:2967–75.
38. Maus MV, Thomas AK, Leonard DG, Allman D, Addya K, Schlienger K, et al. *Ex vivo* expansion of polyclonal and antigen-specific cytotoxic T lymphocytes by artificial APCs expressing ligands for the T-cell receptor, CD28 and 4-1BB. Nat Biotechnol 2002;20:143–8.
39. Suhoski MM, Golovina TN, Aqui NA, Tai VC, Varela-Rohena A, Milone MC, et al. Engineering artificial antigen-presenting cells to express a diverse array of co-stimulatory molecules. Mol Ther 2007;15:981–8.
40. Hirano N, Butler MO, Xia Z, Ansén S, von Bergwelt-Baildon MS, Neuberg D, et al. Engagement of CD83 ligand induces prolonged expansion of CD8$^+$ T cells and preferential enrichment for antigen specificity. Blood 2006;107:1528–36.
41. Neeson P, Shin A, Tainton KM, Guru P, Prince HM, Harrison SJ, et al. *Ex vivo* culture of chimeric antigen receptor T cells generates functional CD8$^+$ T cells with effector and central memory-like phenotype. Gene Ther 2010;17:1105–16.
42. Zeng R, Spolski R, Finkelstein SE, Oh S, Kovanen PE, Hinrichs CS, et al. Synergy of IL-21 and IL-15 in regulating CD8$^+$ T cell expansion and function. J Exp Med 2005;201:139–48.
43. Hinrichs CS, Spolski R, Paulos CM, Gattinoni L, Kerstann KW, Palmer DC, et al. IL-2 and IL-21 confer opposing differentiation programs to CD8$^+$ T cells for adoptive immunotherapy. Blood 2008;111:5326–33.
44. Schluns KS, Lefrancois L. Cytokine control of memory T-cell development and survival. Nat Rev Immunol 2003;3:269–79.
45. Kim YS. Tumor therapy applying membrane-bound form of cytokines. Immune Netw 2009;9:158–68.
46. Cimino AM, Palaniswami P, Kim AC, Selvaraj P. Cancer vaccine development: protein transfer of membrane-anchored cytokines and immunostimulatory molecules. Immunol Res 2004;29:231–40.
47. Wu Z, Xu Y. IL-15R alpha-IgG1-Fc enhances IL-2 and IL-15 anti-tumor action through NK and CD8$^+$ T cells proliferation and activation. J Mol Cell Biol 2010;2:217–22.
48. Fujisaki H, Kakuda H, Imai C, Mullighan CG, Campana D. Replicative potential of human natural killer cells. Br J Haematol 2009;145:606–13.
49. Gong W, Xiao W, Hu M, Weng X, Qian L, Pan X, et al. *Ex vivo* expansion of natural killer cells with high cytotoxicity by K562 cells modified to co-express major histocompatibility complex class I chain-related protein A, 4–1BB ligand, and interleukin-15. Tissue Antigens 2010;76:467–75.